Effect of cooperative grain boundary sliding and migration on emission of dislocations from a crack tip in nanocrystalline materials

H. Feng [1], Q.H. Fang [1, 2,*], Y.W. Liu [1]

1 State Key Laboratory of Advanced Design and Manufacturing for Vehicle Body (Hunan University), Changsha 410082, China
2 School of Mechanical and Manufacturing Engineering, The University of New South Wales, NSW 2052, Australia
* Corresponding author: fangqh1327@tom.com ; Qi-hong.fang@unsw.edu.au

Abstract Interaction of the cooperative grain boundary sliding and migration with a crack in deformed nanocrystalline materials is investigated using the complex variable method. Effects of the two disclination dipoles produced by the cooperative deformation on the emission of lattice dislocations from the crack tip are theoretically described. The complex form expressions of the stress field and the force field are divided. The critical stress intensity factors for the first dislocation emission are calculated. Influences of disclination strength, grain size, locations of the two disclination dipoles as well as crack length on the critical stress intensity factors are discussed in detail. Results show that, the cooperative deformation has great influence on dislocation emission from the crack tip. In general, the cooperative deformation can promote the lattice dislocation emission from the crack tip, thus improve the toughness of the nanocrystalline materials.
Keywords nanocrystalline materials; crack; grain boundary sliding; grain boundary migration; dislocation emission;

1. Introduction

Nanocrystalline metals and ceramics show outstanding mechanical and physical properties, which represent the subject of rapidly growing research efforts motivated by a wide range of their applications [1-8]. However, in most cases, nanocrystalline materials have superior strength, hardness and good wear resistance but at the expenses of both low tensile ductility and low fracture toughness, which considerably limit their practical utility [3-5, 9-11]. At the same time, there are several examples of nanocrystalline materials showing considerable tensile ductility at room temperatures [4, 12-14], or superplasticity at elevated temperatures [14, 15], and significant fracture toughness that can be often higher than that of their polycrystalline or singlecrystalline counterparts [4, 16-19]. The nature of the outstanding combination of good ductility and superior strength is not quite clear, which creates high interest in understanding the toughening mechanisms that specific for nanocrystalline materials. Recently, many models have been developed to explain this phenomenon. In most of them, intergrain sliding, grain boundary migration, triple junction diffusional creep, Coble creep, rotational deformation and nanoscale deformation twinning have been theoretically described as specific deformation modes in nanocrystalline materials. And the specific toughening mechanisms are attributed to specific deformation modes in nanocrystalline materials [20-25].

Recently, rapidly growing attention has been focused on a new physical mechanism or mode of plastic deformation in nanocrystalline metals and ceramics. The new specific deformation mode represents the cooperative grain boundary sliding and stress-driven grain boundary migration process near the tips of growing cracks [26]. Grain boundary sliding is an important deformation mechanism in nanocrystalline materials [3, 4, 10]. It is also one of the specific deformation modes showing superplasticity in nanocrystalline materials [4, 15]. Non-accommodated grain boundary sliding in nanocrystalline solids creates defects (dislocations and disclination dipoles) at triple junctions of grain boundaries. These defects can initiating the formation of cracks, in which case a nanocrystalline solid tends to exhibit brittle behaviour [27, 28]. In contrast, if grain boundary

sliding is effectively accommodated, nanocrystalline solids show enhanced ductility and/or superplasticity [4, 15, 29]. And it is effectively realized that accommodation of grain boundary sliding occurs through lattice dislocation emission from triple junctions, diffusion, and rotational deformation [4, 15, 29]. There has been a new way to accommodate grain boundary sliding through grain boundary migration suggested and theoretically analyzed [20, 26]. Grain boundary migration is another toughening micromechanism [30] and specific deformation mode in nanocrystalline materials [3, 22].

The new accommodation mode we discussed above involving the cooperative grain boundary sliding and stress-driven grain boundary migration, servers as a special deformation mode enhanced compared to pure grain boundary sliding in nanocrystalline materials [20]. In the cooperative process, defects created by grain boundary sliding are, in part, accommodated by defects created by grain boundary migration. The cooperative grain boundary sliding and migration has been theoretically described as a deformed mode operation in crack-free nanocrystalline materials in Bobylev et al. [20]. And it is theoretically revealed that the mode enhances the ductility of nanocrystalline solids in wide ranges of their structural parameters. In the work of Ovid'ko et al. [26], the cooperative grain boundary sliding and migration process near crack tips has been described, and its effect on the fracture toughness of nanocrystalline materials has been theoretically analyzed. The results show that the mechanism considerably enhances the fracture toughness of nanocrystalline materials.

The previous works have lots of experimental and theoretical results suggest that the cooperative grain boundary sliding and migration serving as a special deformation contributes to the toughening of nanocrystalline materials [20, 26]. But the effect of the cooperative grain boundary sliding and migration on the emission of lattice dislocations from crack tips has not been well quantitatively studied. Considering nanocrystalline solids with cracks, if the stress intensity near the crack tip is large enough, the crack can induce plastic shear through the emission of lattice dislocations from the crack tip. The emission of dislocations from cracks causes effective blunting of cracks, thus suppresses their growth, improves the toughness of nanocrystalline materials. So the crack blunting and growth processes are controlled by dislocation emission from crack tips. In the context discussed, there is large interest in the effect of the cooperative mode on lattice dislocation emission from crack tips. The main aim of the paper is to study the effect of the cooperative grain boundary sliding and migration on lattice dislocation emission from the crack tip using a theoretical mode.

2. Model and problem formulation

Let us consider a deformed nanocrystalline solid with a crack under remote mode I loadings and remote mode II loadings. The solid is supposed to be an elastically isotropic solid characterized by the shear modulus μ and Poisson's ratio ν. For definiteness, referring to the approximation in Ovid'ko et al. [26], we will focus our analysis on the situation where the crack is flat and plane, and characterized by the length L. For simplicity, we assume that the defect structure of the solid is the same along the coordinate axis z perpendicular to the xy plane. This assumption will allow us to simplify the mathematical analysis of the problem in our study, reducing it to the consideration of a two-dimensional structure. At the same time, the two-dimensional description definitely reflects the key aspects of the problem.

The applied loadings and high stress concentration near the crack tip can induce both grain boundary sliding and migration near this crack tip. And the geometry of the cooperative grain boundary sliding and migration deformation is schematically presented in Fig. 1. Fig. 1a depicts a deformed nanocrystalline solid with a flat crack. The formation of two disclination dipoles CD and BE results from the cooperative grain boundary sliding and migration process and the dislocation emission is shown in Fig. 1b [26].

Within the model, the vertical grain boundary AB is assumed to be normal to the crack growth direction and make an angle φ with the grain boundaries AA_1 and BB_2. Let the triple junction

A lie at a vertical distance p and a horizontal distance p' from the crack tip and the length of all grain boundaries in the initial state be denoted as d. The disclination dipole CD of wedge disclinations is characterized by the strength magnitude ω and the arm $|x-y|$. The disclination dipole BE is characterized by the strength magnitude ω and the arm y. And x, y denote the distances of the grain boundary sliding and migration.

Let us introduce a Cartesian system (x,y) and a polar coordinate system (r,θ) with the origins at the point O. Then, the coordinates of the disclinations located at the points D, C, E and B can be described as $z_1\ (=r_1 e^{i\theta_1})$, $z_2\ (=r_2 e^{i\theta_2})$, $z_3\ (=r_3 e^{i\theta_3})$ and $z_4\ (=r_4 e^{i\theta_4})$, respectively. And the coordinates (r_j,θ_j) are calculated as follows:

$r_1(y)=\sqrt{y^2+p^2-2yp\cos\varphi}$, $r_2(x)=\sqrt{x^2+p^2-2xp\cos\varphi}$, $r_3(y)=\sqrt{y^2+(p+d)^2-2y(p+d)\cos\varphi}$, $r_4=p+d$;
$\theta_1(y)=-\arccos(y\sin\varphi/r_1)$, $\theta_2(x)=-\arccos(x\sin\varphi/r_2)$, $\theta_3(y)=-\arccos(y\sin\varphi/r_3)$, $\theta_4=-\pi/2$.

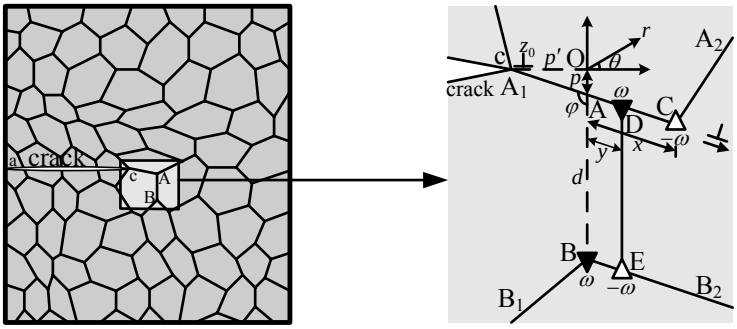

(a) (b)

Fig. 1 The cooperative grain boundary sliding and migration in a deformed nanocrystalline solid with a crack (a) General view. (b) The formation of two disclination dipoles CD and BE results from the cooperative grain boundary sliding and migration process, and the dislocation emission from the crack tip.

Now, let us calculate the stress fields produced by the cooperative grain boundary sliding and migration in the deformed nanocrystalline solid with a flat crack.

For the plane strain problem, stress fields (σ_{xx}, σ_{xy} and σ_{yy}) and displacement fields (u_x and u_y) may be expressed in terms of two Muskhelishvili's complex potentials $\Phi(z)$ and $\Psi(z)$ in the complex plane $z=x+\mathrm{i}y$: [31]

$$\sigma_{xx}+\sigma_{yy}=2\left(\Phi(z)+\overline{\Phi(z)}\right), \tag{1}$$

$$\sigma_{yy}-\mathrm{i}\sigma_{xy}=\Phi(z)+\overline{\Phi(z)}+z\overline{\Phi'(z)}+\overline{\Psi(z)}, \tag{2}$$

$$2\mu\left(u_x'+u_y'\right)=(3-4\nu)\Phi(z)-\overline{\Phi(z)}-z\overline{\Phi'(z)}-\Psi(z), \tag{3}$$

where $u_x'=\partial u_x/\partial x$, $u_y'=\partial u_y/\partial x$, $\Phi'(z)=\mathrm{d}\left[\Phi(z)\right]/\mathrm{d}z$, the over-bar represents the complex conjugate.

And the stress fields can be written as

$$\sigma_{xx}=\mathrm{Re}\left[2\Phi(z)-\bar{z}\Phi'(z)-\Psi(z)\right], \tag{4}$$

$$\sigma_{xy}=\mathrm{Im}\left[\bar{z}\Phi'(z)+\Psi(z)\right], \tag{5}$$

$$\sigma_{yy}=\mathrm{Re}\left[2\Phi(z)+\bar{z}\Phi'(z)+\Psi(z)\right]. \tag{6}$$

The boundary condition of the crack for the present problem can be expressed as

$$\sigma_{yy}(t)-\mathrm{i}\sigma_{xy}(t)=0,\quad t\in\text{crack}. \tag{7}$$

According the Romanov and Vladimirov [32], the elastic stress fields produced by a wedge disclination characterized by strength ω, located at the point z_k $(=x_k+\mathrm{i}y_k)$ in an infinite homogeneous medium may be expressed as follows:

$$\sigma_{xx}=\frac{\mu\omega}{2\pi(1-\nu)}\left(\frac{1}{2}\ln\left((x-x_k)^2+(y-y_k)^2\right)+\frac{(y-y_k)^2}{(x-x_k)^2+(y-y_k)^2}\right), \tag{8}$$

$$\sigma_{xy}=-\frac{\mu\omega}{2\pi(1-\nu)}\frac{(x-x_k)(y-y_k)}{(x-x_k)^2+(y-y_k)^2}, \tag{9}$$

$$\sigma_{yy}=\frac{\mu\omega}{2\pi(1-\nu)}\left(\frac{1}{2}\ln\left((x-x_k)^2+(y-y_k)^2\right)+\frac{(x-x_k)^2}{(x-x_k)^2+(y-y_k)^2}\right). \tag{10}$$

Assume that the elastic fields produced by the cooperative grain boundary sliding and migration in an infinite homogeneous medium can be evaluated by using two complex potentials $\Phi_{\Delta 0}(z)$ and $\Psi_{\Delta 0}(z)$.

Substituting Eqs. (8) and (9) into formula (1), Eqs. (9) and (10) into formula (2), referring to the work in Muskhelishvili [31], Fang et al. [33] and Liu et al. [34], the complex potentials $\Phi_{\Delta 0}(z)$ and $\Psi_{\Delta 0}(z)$ can be taken in the forms:

$$\Phi_{\Delta 0}(z)=\frac{\mu\omega}{4\pi(1-\nu)}\sum_{k=1}^{4}s_k\ln(z-z_k), \tag{11}$$

$$\Psi_{\Delta 0}(z)=-\frac{\mu\omega}{4\pi(1-\nu)}\sum_{k=1}^{4}s_k\frac{\overline{z}_k}{z-z_k}. \tag{12}$$

where $s_k\ (k=1,2,3,4)$ denote the sign of a specified disclination and are defined as $s_1=s_4=1$, $s_2=s_3=-1$.

From Eqs. (11) and (12) together with formulae (1) and (2), we obtain the stress fields which are identical to the results in Eqs. (8)-(10). Eqs. (11) and (12) are singularity principal parts of complex potentials on the problem of the cooperative grain boundary sliding and migration in an infinite homogeneous medium without the crack.

For the problem shown in Fig. 1, the complex potentials $\Phi_{\Delta}(z)$ and $\Psi_{\Delta}(z)$ can be written an

$$\Phi_{\Delta}(z)=\Phi_{\Delta 0}(z)+\Phi_{\Delta}^{*}(z), \tag{13}$$

$$\Psi_{\Delta}(z)=\Psi_{\Delta 0}(z)+\Psi_{\Delta}^{*}(z), \tag{14}$$

where $\Phi_{\Delta 0}(z)$ and $\Psi_{\Delta 0}(z)$ indicate the terms due to the presence of the cooperative grain boundary sliding and migration located in infinite medium, and $\Phi_{\Delta}^{*}(z)$ and $\Psi_{\Delta}^{*}(z)$ refer to the terms resulting from the interaction of the cooperative grain boundary sliding and migration with the crack, which are holomorphic in the region.

By using Riemann-Schwarz's symmetry principle, we introduce a new analytical function

$$\Omega_{\Delta}(z)=-\overline{\Phi}_{\Delta}(z)-z\overline{\Phi}'_{\Delta}(z)-\overline{\Psi}_{\Delta}(z). \tag{15}$$

The substitution of Eqs. (13) and (14) into Eq. (15) yields

$$\Omega_{\Delta}(z)=-\frac{\mu\omega}{4\pi(1-\nu)}\sum_{k=1}^{4}s_k\left(\ln(z-\overline{z}_k)+\frac{z-z_k}{z-\overline{z}_k}\right)+\Omega_{\Delta}^{*}(z), \tag{16}$$

where $\Omega_{\Delta}^{*}(z)$ is holomorphic in the region.

Considering the above complex potentials, the crack boundary condition (7) can be written an

$$\left[\Phi_{\Delta}(t)-\Omega_{\Delta}(t)\right]^{+}+\left[\Phi_{\Delta}(t)-\Omega_{\Delta}(t)\right]^{-}=0,\quad t\in\text{crack}, \tag{17}$$

$$\left[\Phi_{\Delta}(t)-\Omega_{\Delta}(t)\right]^{+}-\left[\Phi_{\Delta}(t)-\Omega_{\Delta}(t)\right]^{-}=0,\quad t\in\text{crack}, \tag{18}$$

where the superscripts "$+$" and "$-$" denote the boundary values of the physical quantity as z approached the crack from the upper half plane and the lower half plane.

Without loss in generality, we assume that two ends of the crack are located at points a and c on the x-axis. Therefore, the complex potentials $\Phi_{\Delta}(z)$ and $\Psi_{\Delta}(z)$ have the following forms:

$$\Phi_{\Delta}(z)=\frac{\mu\omega}{8\pi(1-\nu)}\sum_{k=1}^{4}s_k\left(\ln\frac{z-z_k}{z-\overline{z}_k}-\frac{z-z_k}{z-\overline{z}_k}\right)$$
$$+\frac{\mu\omega}{8\pi(1-\nu)}X_0(z)\sum_{k=1}^{4}s_k\left(\frac{1}{X_0(z_k)}\ln(z-z_k)-z_k+\overline{z}_k-\frac{1}{X_0(\overline{z}_k)}\left(\frac{z-z_k}{z-\overline{z}_k}+\ln(z-\overline{z}_k)\right)\right), \tag{19}$$

$$\Psi_{\Delta}(z)=\frac{\mu\omega}{8\pi(1-\nu)}\sum_{k=1}^{4}s_k\left(\frac{3z-z_k}{z-\overline{z}_k}-\frac{\overline{z}_k}{z-z_k}-\frac{z(z-z_k)}{(z-\overline{z}_k)^2}\right)-\frac{\mu\omega}{8\pi(1-\nu)}X_0(z)\sum_{k=1}^{4}s_k\left(\frac{1}{X_0(z_k)}\frac{\overline{z}_k}{z-z_k}+\frac{1}{X_0(\overline{z}_k)}\left(\frac{z(z-z_k)}{(z-\overline{z}_k)^2}-\frac{3z-z_k}{z-\overline{z}_k}\right)\right)$$
$$-\frac{\mu\omega}{8\pi(1-\nu)}X_0'(z)\sum_{k=1}^{4}s_k\left(\frac{1}{X_0(z_k)}z\ln(z-z_k)-z(z-\overline{z}_k)-\frac{1}{X_0(\overline{z}_k)}z\left(\frac{z-z_k}{z-\overline{z}_k}+\ln(z-\overline{z}_k)\right)\right), \tag{20}$$

where $X_0(z)=1\Big/\sqrt{(z-a)(z-c)}$, $X_0'(z)=\mathrm{d}X_0(z)/\mathrm{d}z$.

Substituting Eqs. (19) and (20) into formulae (4), (5) and (6), we obtain the stress fields due to the cooperative grain boundary sliding and migration.

3. The emission force of lattice dislocations

Let us consider the emission of lattice dislocations from the crack tip. For simplicity, we focus on the situation where the dislocations are of edge character and their Burgers vectors lie along the slip plane that makes an angle θ with the x-axis.

For the first dislocation located at $z_0=r_0\mathrm{e}^{\mathrm{i}\theta_0}$ in the coordination system, the elastic fields can be evaluated by using the complex potentials $\Phi_{\perp}(z)$, $\Psi_{\perp}(z)$ and $\Omega_{\perp}(z)$.

Referring to the work in Fang et al. [35-37], the complex potentials can be expressed as:
$\Phi_{\perp}(z)=\Phi_{\perp 0}(z)+\Phi_{\perp}^{*}(z)$, $\Psi_{\perp}(z)=\Psi_{\perp 0}(z)+\Psi_{\perp}^{*}(z)$,

where $\Phi_{\perp 0}(z)=\dfrac{w}{z-z_0}$ and $\Psi_{\perp 0}(z)=\dfrac{\overline{w}}{z-z_0}+\dfrac{w\overline{z}_0}{(z-z_0)^2}$.

Using the same method in the section 2, we can obtain

$$\Phi_{\perp}(z)=\frac{1}{2}\left(\frac{w}{z-z_0}-\frac{w}{z-\overline{z}_0}-\frac{\overline{w}(z_0-\overline{z}_0)}{(z-\overline{z}_0)^2}\right)$$
$$+\frac{1}{2}X_0(z)\left(\frac{1}{X_0(z_0)}\frac{w}{z-z_0}+\frac{1}{X_0(\overline{z}_0)}\frac{w}{z-\overline{z}_0}+\frac{1}{X_0(\overline{z}_0)}\frac{\overline{w}(z_0-\overline{z}_0)}{(z-\overline{z}_0)^2}+X_0(\overline{z}_0)\frac{\overline{w}\overline{z}_0(z_0-\overline{z}_0)}{z-\overline{z}_0}\right), \tag{21}$$

$$\Omega_{\perp}(z)=\frac{1}{2}\left(\frac{w}{z-z_0}-\frac{w}{z-\overline{z}_0}-\frac{\overline{w}(z_0-\overline{z}_0)}{(z-\overline{z}_0)^2}\right)$$
$$-\frac{1}{2}X_0(z)\left(\frac{1}{X_0(z_0)}\frac{w}{z-z_0}+\frac{1}{X_0(\overline{z}_0)}\frac{w}{z-\overline{z}_0}+\frac{1}{X_0(\overline{z}_0)}\frac{\overline{w}(z_0-\overline{z}_0)}{(z-\overline{z}_0)^2}+X_0(\overline{z}_0)\frac{\overline{w}\overline{z}_0(z_0-\overline{z}_0)}{z-\overline{z}_0}\right), \tag{22}$$

$$\Psi_{\perp}(z)=-\Phi_{\perp}(z)-z\Phi_{\perp}'(z)-\overline{\Omega}_{\perp}(z), \tag{23}$$

where $w=\dfrac{\mu}{4\pi(1-\nu)}(b_y-\mathrm{i}b_x)$.

The above complex potentials $\Phi_{\perp 0}(z)$ and $\Phi_{\perp}^{*}(z)$ are consistent with the complex functions ϕ_d' and $\phi_i'(z)$ in Zhang and Li [38].

Then, the force acting on the edge dislocation consists of three parts: the image force, the force produced by the cooperative grain boundary sliding and migration and the external force.

Firstly, using the Peach-Koehler formula [39], the image force can be written as

$$f_{\perp}=f_x-\mathrm{i}f_y=\left[\overset{\curvearrowright}{\sigma}_{xy}(z_0)b_x+\overset{\curvearrowright}{\sigma}_{yy}(z_0)b_y\right]+\mathrm{i}\left[\overset{\curvearrowright}{\sigma}_{xx}(z_0)b_x+\overset{\curvearrowright}{\sigma}_{xy}(z_0)b_y\right]$$

$$= \frac{\mu b^2}{\pi(1+\kappa)}\left(\frac{\Phi_\perp^*(z_0)+\overline{\Phi_\perp^*(z_0)}}{w}+\frac{\overline{z}_0\Phi_\perp^{*\prime}(z_0)+\Psi_\perp^*(z_0)}{\overline{w}}\right) \tag{24}$$

where σ'_{xx}, σ'_{xy} and σ'_{yy} are the components of the perturbation stress, and

$$\Phi_\perp^*(z_0)=\lim_{z\to z_0}\left(\Phi_\perp(z)-\Phi_{\perp 0}(z)\right),\quad \Phi_\perp^{*\prime}(z_0)=\lim_{z\to z_0}\frac{\mathrm{d}\left(\Phi_\perp(z)-\Phi_{\perp 0}(z)\right)}{\mathrm{d}z},\quad \Psi_\perp^*(z_0)=\lim_{z\to z_0}\left(\Psi_\perp(z)-\Psi_{\perp 0}(z)\right).$$

Then, the force produced by the cooperative grain boundary sliding and migration can be written as [39]

$$\begin{aligned} f_\Delta &= f_x - \mathrm{i}f_y = \left[\sigma_{xy}(z_0)b_x+\sigma_{yy}(z_0)b_y\right]+\mathrm{i}\left[\sigma_{xx}(z_0)b_x+\sigma_{xy}(z_0)b_y\right] \\ &= \frac{\mu b^2}{\pi(1+\kappa)}\left(\frac{\Phi_\Delta(z_0)+\overline{\Phi_\Delta(z_0)}}{w}+\frac{\overline{z}_0\Phi_\Delta'(z_0)+\Psi_\Delta(z_0)}{\overline{w}}\right), \end{aligned} \tag{25}$$

where σ_{xx}, σ_{xy} and σ_{yy} are the components of the stress fields produced by the cooperative grain boundary sliding and migration.

Lastly, the external force acting on the edge dislocation can be written as (Fang et al., 2012)

$$f_\Gamma = b\sigma_{r\theta}=\frac{b}{\sqrt{2\pi r}}\left(\frac{1}{2}\sin\theta\cos\frac{\theta}{2}K_{\mathrm{I}}^{app}+\left(\cos\frac{3\theta}{2}+\sin^2\frac{\theta}{2}\cos\frac{\theta}{2}K_{\mathrm{II}}^{app}\right)\right), \tag{26}$$

where $\sigma_{r\theta}$ is the in-plane shear stress due to the applied model I and mode II stress intensity factors, K_{I}^{app} and K_{II}^{app} are the generalized mode I and mode II stress intensity factors produced by the remote loadings.

Then, the dislocation emission force acting on the edge dislocation can be written as

$$f_{emit} = f_x\cos\theta + f_y\sin\theta + f_\Gamma = \mathrm{Re}\left[f_\perp + f_\Delta\right]\cos\theta - \mathrm{Im}\left[f_\perp + f_\Delta\right]\sin\theta + f_\Gamma \tag{27}$$

Substituting Eqs. (24), (25) and (26) into the Eq. (27), we have the expression of the dislocation emission force.

4. The critical stress intensity factors for the dislocation emission

A commonly accepted criterion for the emission of dislocations from a crack tip is, when the force acts on them, is equal to zero. Moreover, the dislocation distance to the crack surface must be equal to, or larger than, the dislocation core radius [40]. Combining expressions (24)-(27) and $f_{emit}=0$ yields the critical stress intensity factor K_{IC}^{app} and K_{IIC}^{app} for the dislocation emission as follows. We discuss the effects of the cooperative grain boundary sliding and migration on the emission of lattice dislocations from the crack tip.

$$K_{\mathrm{II}}^{app}=0,\quad K_{\mathrm{IC}}^{app}=\frac{2\sqrt{2\pi r_0}}{b\sin\theta\cos(\theta/2)}\left(\mathrm{Im}\left[f_\perp+f_\Delta\right]\sin\theta-\mathrm{Re}\left[f_\perp+f_\Delta\right]\cos\theta\right),$$

$$K_{\mathrm{I}}^{app}=0,\quad K_{\mathrm{IIC}}^{app}=\frac{\sqrt{2\pi r_0}}{b\left(\cos(3\theta/2)+\sin^2(\theta/2)\cos(\theta/2)\right)}\left(\mathrm{Im}\left[f_\perp+f_\Delta\right]\sin\theta-\mathrm{Re}\left[f_\perp+f_\Delta\right]\cos\theta\right),$$

where $f_\perp+f_\Delta=\dfrac{\mu b^2}{\pi(1+\kappa)}\left(\dfrac{2\,\mathrm{Re}\left[\Phi_\perp^*(z_0)+\Phi_\Delta(z_0)\right]}{w}+\dfrac{\overline{z}_0\left(\Phi_\perp^{*\prime}(z_0)+\Phi_\Delta'(z_0)\right)+\Psi_\perp^*(z_0)+\Psi_\Delta(z_0)}{\overline{w}}\right)$.

Let us calculate the critical stress intensity factors K_{IC}^{app} and K_{IIC}^{app} in the situation, where the cooperative grain boundary sliding and migration forms near the crack tip, as shown in Fig. 1. We define the critical normalized stress intensity factors (SIFs) as $K_{\mathrm{IC}}^0=K_{\mathrm{IC}}^{app}/\mu\sqrt{b}$ and $K_{\mathrm{IIC}}^0=K_{\mathrm{IIC}}^{app}/\mu\sqrt{b}$.

We use the following typical values of parameters of the nanocrystalline material Ni: $\mu=73\,\mathrm{Gpa}$, $\nu=0.31$ [41]. We assume that the crack tip located at the coordinate origin, the Burgers vector of the edge dislocation $b=0.25\,\mathrm{nm}$ and the dislocation core radius $r_0=b/2$.

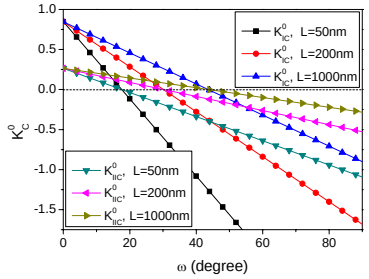

Fig. 2 Dependences of the critical normalized SIFs K_{C}^{0} on the disclination strength ω with different crack lengths L ($\varphi=2\pi/3$, $\theta_0=\pi/6$, $d=15\,\mathrm{nm}$, $p=0$, $x/d=0.3$, $y/d=0.1$)

With different crack lengths L, the variations of the critical normalized stress intensity factors (SIFs) K_{IC}^{0} and K_{IIC}^{0} with respect to the disclination strength ω are respectively shown in Fig. 2. We found that the critical normalized SIFs K_{IC}^{0} and K_{IIC}^{0} both decrease with the increment of the disclination strength ω. With the same crack length L, the critical normalized SIFs K_{IC}^{0} and K_{IIC}^{0} have an intersection at the critical point ω_0, where the critical normalized SIFs equal to zero. When the disclination strength is larger than the critical value ω_0, the dislocation can emit from the crack tip without any external loadings. And the critical value ω_0 will increase with increasing of the crack length L. So the cooperative grain boundary sliding and migration can promote the dislocation emission from the crack tip, thus improve the toughness of the nanocrystalline materials. We can also see that, with the same disclination strength and the same crack length, the critical normalized SIF K_{IIC}^{0} is much smaller than K_{IC}^{0}, which means the mode II loadings are easier than the mode I loadings to make the dislocation emit form the crack tip.

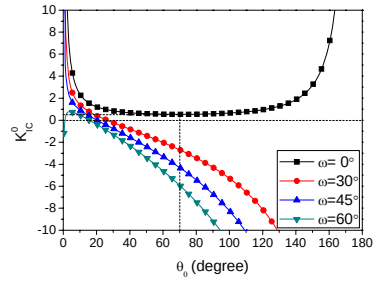

Fig. 3 Dependences of the critical normalized SIFs K_{IC}^{0} on the edge dislocation emission angle θ_0 ($\varphi=2\pi/3$, $L=100\,\mathrm{nm}$, $d=15\,\mathrm{nm}$, $p=0$, $x/d=0.3$, $y/d=0.1$)

The critical normalized SIFs versus the dislocation emission angle θ_0 with different disclination strengths ω are depicted in Fig. 3 and Fig. 4. We can see that, the critical normalized SIFs have totally different variation tendency compared to the situation that the cooperative grain boundary sliding and migration is vanished ($\omega=0°$). For the model I stress intensity factors in Fig. 3, the critical normalized SIF firs decrease then increase with increasing of the edge dislocation emission angle when the cooperative grain boundary sliding and migration does not exist ($\omega=0°$). And in this case, the most probable angle for the edge dislocation emission is $70.53°$, which is in good agreement with the result in Huang and Li [42]. But for the disclination strength $\omega=30°$ and $45°$, the critical normalized SIFs K_{IC}^{0} sharply decrease with increasing of the dislocation emission angle, and transfer the positive dislocations emission to the negative dislocations emission. And the most probable angle for the dislocation emission is $26.25°$ for $\omega=30°$ and 20.25 for $\omega=45°$, respectively. For the disclination strength $\omega=60°$, the critical normalized SIFs K_{IC}^{0} first increase then decrease with the increment of the dislocation emission angle. There are two most probable angle for the positive dislocation emission, and they are $0.95°$ and $15.75°$.

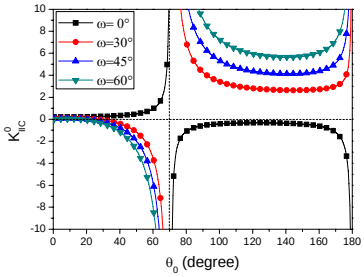

Fig. 4 Dependences of the critical normalized SIFs K^0_{IIC} on the edge dislocation emission angle θ_0 ($\varphi = 2\pi/3$, $L = 100\,\mathrm{nm}$, $d = 15\,\mathrm{nm}$, $p = 0$, $x/d = 0.3$, $y/d = 0.1$)

For the mode II stress intensity factors in Fig. 4, when the cooperative grain boundary sliding and migration does not exist ($\omega = 0°$), the critical normalized SIFs increase from a finite positive value to infinity with increasing of the edge dislocation emission angle, then switch to negative value. And the most probable angle for the positive dislocation emission is $0°$, that for the negative dislocation is $123.75°$. In other cases, the critical normalized SIFs decrease from finite negative values to infinity, then switch to positive values with the increment of the dislocation emission angle. And the most probable angle for the negative dislocation emission is always $0°$, that for the positive dislocation is $144.25°$ for $\omega = 30°$, $141.25°$ for $\omega = 45°$, and 139.75 for $\omega = 60°$.

The dependences of the critical normalized SIFs on the dislocation emission angle with different ratios x/d and y/d are shown in Figs. 5-6. We can see that, the critical normalized SIFs versus the dislocation emission angle have different variation tendency depending on the values of the ratios x/d and y/d. It is not only we described above.

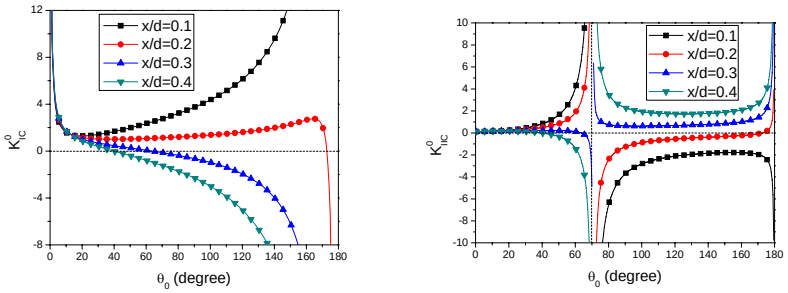

Fig. 5 Dependences of the critical normalized SIFs K^0_{C} on the dislocation emission angle θ_0 with different ratio x/d ($\omega = \pi/6$, $\varphi = 2\pi/3$, $L = 100\,\mathrm{nm}$, $d = 15\,\mathrm{nm}$, $p = 0$, $y/d = 0.3$)

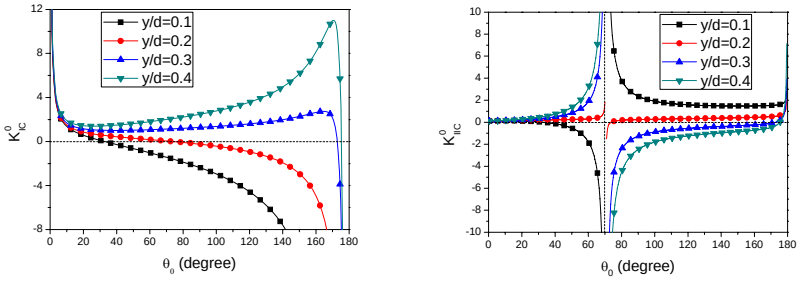

Fig. 6 Dependences of the critical normalized SIFs K^0_{C} on the dislocation emission angle θ_0 with different ratio y/d ($\omega = \pi/6$, $\varphi = 2\pi/3$, $L = 100\,\mathrm{nm}$, $d = 15\,\mathrm{nm}$, $p = 0$, $x/d = 0.2$)

The critical normalized SIFs K^0_{IC} versus the grain size d with different angles φ between grain boundaries are depicted in Fig. 7. It indicates that the critical normalized SIFs first increase then decrease with the increment of the grain size d, but decrease with increasing of the angle φ between grain boundaries. There is a critical grain size making the critical normalized SIFs equal to zero. And when the grain size d is larger than the critical value, the dislocation can emit from the crack tip without any loadings. The critical value also decreases with increasing of the angel φ between grain boundaries.

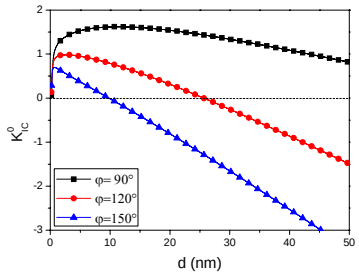

Fig. 7 Dependences of the critical normalized SIFs K_{IC}^0 on the grain size d with different angles φ ($\omega=\pi/6$, $\theta_0=\pi/6$, $L=100\,\mathrm{nm}$, $p=d$, $x/d=0.3$, $y/d=0.1$)

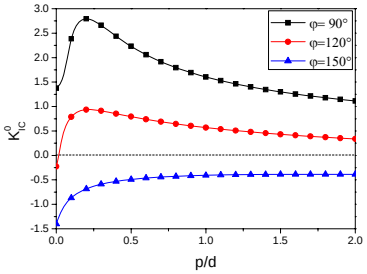

Fig. 8 Dependences of the critical normalized SIFs K_{IC}^0 on the ratio p/d with different angles φ ($\omega=\pi/6$, $\theta_0=\pi/6$, $L=100\,\mathrm{nm}$, $d=15\,\mathrm{nm}$, $x/d=0.3$, $y/d=0.1$)

Fig. 8 plots the variations of the critical normalized SIFs with respect to the ratio p/d with different angles φ between grain boundaries. We found that the critical normalized SIFs first increase then decrease to constants with the increment of the ratio p/d for $\varphi=90°$ and $120°$, but just increase to a constant for $\varphi=150°$. And in this situation, if the angle φ between the grain boundaries is large enough, the critical normalized SIF is always negative, which means the dislocation emission from the crack tip is very easy.

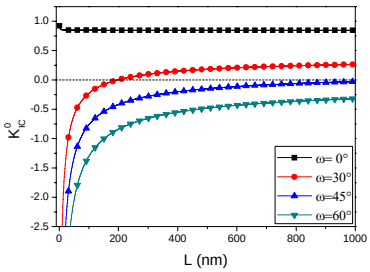

Fig. 9 Dependences of the critical normalized SIFs K_{IC}^0 on the crack length L with different strengths ω ($\theta_0=\pi/6$, $\varphi=2\pi/3$, $d=15\,\mathrm{nm}$, $p=0$, $x/d=0.3$, $y/d=0.1$)

The dependences of the critical normalized SIFs on the crack length with different disclination strengths are shown in Fig. 9. The critical normalized SIFs K_{IC}^0 increase with the increment of the crack length, and tend to constants when the crack length is large enough. So the dislocation emission from the short crack tip is much easier, and growth of the long crack is easier. We can also see that, when the cooperative grain boundary sliding and migration does not exist, the crack length just slightly affects the critical normalized SIFs. In comparison, the cooperative grain boundary sliding and migration contributes a lot to the dislocation emission and the crack blunting.

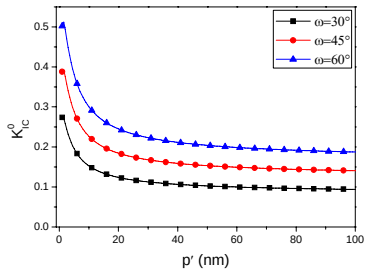

Fig. 10 Dependences of the critical normalized SIFs K_{IC}^{0} on the distance between crack tip and coordinate origin p' ($\theta_0=\pi/6$, $\varphi=2\pi/3$, $L=300\,\mathrm{nm}$, $d=15\,\mathrm{nm}$, $p=0$, $x/d=0.3$, $y/d=0.1$)

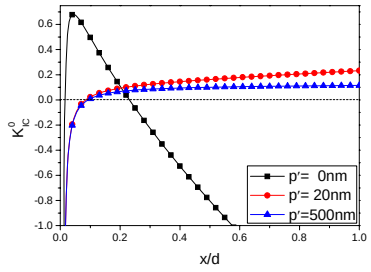

Fig. 11 Dependences of the critical normalized SIFs K_{IC}^{0} on the ratio x/d with different distances p' ($\omega=\pi/6$, $\theta_0=\pi/6$, $\varphi=2\pi/3$, $L=100\,\mathrm{nm}$, $d=15\,\mathrm{nm}$, $p=0$, $y/d=0.1$)

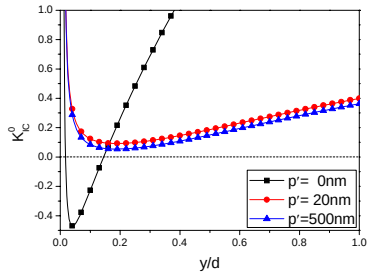

Fig. 12 Dependences of the critical normalized SIFs K_{IC}^{0} on the ratio y/d with different distances p' ($\omega=\pi/6$, $\theta_0=\pi/6$, $\varphi=2\pi/3$, $L=100\,\mathrm{nm}$, $d=15\,\mathrm{nm}$, $p=0$, $x/d=0.3$)

If the crack tip is not at the coordinate origin, we define the horizontal distance between the crack tip and the coordinate origin is p'. Fig. 10 plots the dependences of the critical normalized SIFs on the distance between the crack tip and the coordinate origin p' with different disclination strengths. The critical normalized SIFs decrease and tend to constants with increasing of the distance p'. The variations of the critical normalized SIFs on the ratios x/d and y/d with different distances p' are depicted in Fig. 11 and Fig. 12, respectively. Fig. 11 indicates that the critical normalized SIFs first increase then decrease with the increment of the ratio x/d when the crack tip is at the coordinate origin ($p'=0$), and the change is remarkable. In other cases, the critical normalized SIFs just increase with increasing of the ratio, and the distances p' have slight influence on them. The variation tendency of the critical normalized with respect to the radio y/d is just opposite to that to the radio x/d.

5. Concluding remarks

Thus, the interaction of the cooperative grain boundary sliding and migration with the crack is investigated by the complex variable method. We have theoretically described the effects of the two wedge disclination dipoles produced by the cooperative grain boundary sliding and migration on the emission of edge dislocations from the crack tip in deformed nanocrystalline metals and ceramics. The critical stress intensity factors for the first dislocation emission are calculated. The influence of the disclination strength, the grain size, the location of the two disclination dipoles and the crack length on the critical stress intensity factors is discussed in detail. Some conclusions are summarized as follows.

(1) The cooperative grain boundary sliding and migration can promote the dislocation emission from the crack tip, which causes effective blunting of the crack, thus suppresses its growth, and improves the toughness of nanocrystalline materials.

(2) There is a critical disclination strength value making the critical stress intensity factor equal to zero and the dislocation can emit from the crack tip without any external loadings. And the mode II loadings are easier than the mode I loadings to make the dislocation emit form the crack tip.

(3) The critical stress intensity factor has different variation tendency depending on the disclination strength and the geometry of the two disclination dipoles. For each situation, the most probable emission angles for positive dislocation and negative dislocation are different.

(4) The grain size has great effect on the dislocation emission from the crack tip. The critical stress intensity factors first increase then decrease with increasing of the grain size. And there is a critical grain size making the dislocation can emit from the crack tip without any external loadings.

(5) The dislocation emission from the shorter crack tip is much easier. So, the shorter crack can be easily blunted, and the longer crack tends to grow.

(6) The location and geometry of the cooperative grain boundary sliding and migration have great influence on the critical stress intensity factors.

Acknowledgements

The authors would like to deeply appreciate the support from the NNSFC (11172094 and 11172095) and the NCET-11-0122. The work was also supported by the Fundamental Research Funds for the Central Universities, Hunan University.

References

[1] P. Barai, G.J. Weng, Mechanics of a nanocrystalline coating and grain-size dependence of its plastic strength. Mech Mater, 43 (2011) 496-504.

[2] S.V. Bobylev, A.K. Mukherjee, I.A. Ovid'ko, Emission of partial dislocations from amorphous intergranular boundaries in deformed nanocrystalline ceramics. Scripta Mater, 60(1) (2009) 36-39.

[3] M. Dao, L. Lu, R.J. Asaro, J.T.M. De Hosson, E. Ma, Toward a quantitative understanding of mechanical behavior of nanocrystalline metals. Acta Mater, 55(12) (2007) 4041-4065.

[4] C.C. Koch, I.A. Ovid'ko, S. Seal, S. Veprek, Structural nanocrystalline materials: Fundamentals and Applications, Cambridge University Press, Cambridge, 2007.

[5] M.A. Meyers, A. Mishra, D.J. Benson, Mechanical properties of nanocrystalline materials. Prog Mater Sci, 51 (2006) 427-556.

[6] S.H. Xia, J.T. Wang, A micromechanical model of toughening behavior in the dual-phase composite. Int J Plast, 26 (2010) 1442-1460.

[7] K. Zhou, A.A. Nazarov, M.S. Wu, Competing relaxation mechanisms in a disclinated nanowire: temperature and size effects. Phys Rev Lett, 98 (2007) 035501.

[8] K. Zhou, M.S. Wu, A.A. Nazarov, Relaxation of a disclinated tricrystalline nanowire. Acta Mater, 56 (2008) 5828-5836.

[9] C.C. Koch, Structural nanocrystalline materials: an overview. J Mater Sci, 42(5) (2007) 1403-1414.

[10] I.A. Ovid'ko, Deformation and diffusion modes in nanocrystalline materials. Int Mater Rev, 50 (2005) 65-82.

[11] R.T. Zhu, J.Q. Zhou, H. Jiang, D.S. Zhang, Evolution of shear banding in fully dense nanocrystalline Ni sheet. Mech Mater, 51 (2012) 29-42.

[12] S. Cheng, E. Ma, Y.M. Wang, L.J. Kecskes, K.M. Youssef, C.C. Koch, U.P. Trociewitz, K. Han, Tensile properties of in situ consolidated nanocrystalline Cu. Acta Mater, 53(5) (2005) 1521-1533.

[13] K.M. Youssef, R.O. Scattergood, K.L. Murty, J.A. Horton, C.C. Koch, Ultrahigh strength and high ductility of bulk nanocrystalline copper. Appl Phys Lett, 87 (2005) 091904.

[14] K.M. Youssef, R.O. Scattergood, K.L. Murty, C.C. Koch, Nanocrystalline Al-Mg alloy with ultrahigh strength and good ductility. Scripta Mater, 54(2) (2006) 251-256.

[15] A.V. Sergueeva, N.A. Mara, A.K. Mukherjee, Grain boundary sliding in nanomaterials at elevated temperatures. J Mater Sci, 42(5) (2007) 1433-1438.

[16] S. Bhaduri, S.B. Bhaduri, Enhanced low temperature toughness of Al_2O_3-ZnO_2 nano/nano composites. Nanostruct Mater, 8(6) (1997) 755-763.

[17] A.A. Kaminskii, M.S. Akchurin, R.V. Gainutdinov, K. Takaichi, A. Shirakava, H. Yagi, T. Yanagitani, K. Ueda, Microhardness and fracture toughness of Y_2O_3- and $Y_3Al_5O_{12}$- based nanocrystalline laser ceramics. Crystallogr Rep, 50(5) (2005) 569-873.

[18] R.A. Mirshams, C.H. Xiao, S.H. Whang, W.M. Yin, R-Curve characterization of the fracture toughness of nanocrystalline nickel thin sheets. Mater Sci Eng A, 315(1-2) (2001) 21-27.

[19] Y. Zhao, J. Qian, L.L. Daemen, C. Pantea, J. Zhang, G.A. Voronin, T.W. Zerda, Enhancement of fracture toughness in nanostructured diamond-SiC composites. Appl Phys Lett, 84 (2004) 1356.

[20] S.V. Bobylev, N.F. Morozov, I.A. Ovid'ko, Cooperative grain boundary sliding and migration process in nanocrystalline solids. Phys Rev Lett, 105 (2010) 055504.
[21] S.V. Bobylev, N.F. Morozov, I.A. Ovid'ko, Cooperative grain boundary sliding and nanograin nucleation process in nanocrystalline, ultrafine-grained, and polycrystalline solids. Phys Rev B, 84 (2011) 094103.
[22] M.Yu. Gutkin, I.A. Ovid'ko, Grain boundary migration and rotational deformation mode in nanocrystalline materials. Appl Phys Lett, 87 (2005) 251916.
[23] P.A. Juan, S. Berbenni, L. Capolungo, Prediction of internal stresses during growth of first- and second-generation twins in Mg and Mg alloys. Acta Mater, 60 (2012) 476-486.
[24] N.F. Morozov, I.A. Ovid'ko, A.G. Sheinerman, E.C. Aifantis, Special rotational deformation as a toughening mechanism in nanocrystalline solids. J Mech Phys Solids, 58 (2010) 1088-1099.
[25] I.A. Ovid'ko, A.G. Sheinerman, Ductile vs. brittle behavior of pre-cracked nanocrystalline and ultrafine-grained materials. Scripta Mater, 58 (2010) 5286-5294.
[26] I.A. Ovid'ko, A.G. Sheinerman, E.C. Aifantis, Effect of cooperative grain boundary sliding and migration on crack growth in nanocrystalline solids. Acta Mater, 59 (2011) 5023-5031.
[27] I.A. Ovid'ko, A.G. Sheinerman, Special strain hardening mechanism and nanocrack generation in nanocrystalline materials. Appl Phys Lett, 90(17) (2007) 171927.
[28] I.A. Ovid'ko, A.G. Sheinerman, Enhanced ductility of nanomaterials through optimization of grain boundary sliding and diffusion processes. Acta Mater, 57(7) (2009) 2217-2228.
[29] A.V. Sergueeva, N.A. Mara, N.A. Krasilnikov, R.Z. Valiev, A.K. Mukherjee, Cooperative grain boundary sliding in nanocrystalline materials. Philos Mag, 86(36) (2006) 5797-5804.
[30] I.A. Ovid'ko, A.G. Sheinerman, E.C. Aifantis, Stress-driven migration of grain boundaries and fracture processes in nanocrystalline ceramics and metals. Acta Mater, 56(12) (2008) 2718-2727.
[31] N.L. Muskhelishvili, Soma basic problems of mathematical theory of elasticity, Leyden, Noordhoff, 1975.
[32] A.E. Romanov, V.I. Vladimirov, Disclinations in crystalline solids, in: Nabarro, F.R.N., Dislocation in solids, Amsterdam, Elsevier, 1992, pp. 191-402.
[33] Q.H. Fang, Y.W. Liu, C.P. Jiang, B. Li, Interaction of a wedge disclination dipole with interfacial cracks. Eng Fract Mech, 73 (2006) 1235-1248.
[34] Y.W. Liu, Q.H. Fang, C.P. Jiang, A wedge disclination dipole interaction with a circular inclusion. Phys Stat Sol (A), 203(3) (2006) 443-458.
[35] Q.H. Fang, Y.W. Liu, C.P. Jiang, Edge dislocation interacting with an interfacial crack along a circular inhomogeneity. Int J Solids Struct, 40 (2003) 5781-5797.
[36] Q.H. Fang, Y.W. Liu, B. Jin, P.H. Wen, Effect of interface stressed on the image force and stability of an edge dislocation inside a nanoscale cylindrical inclusion. Int J Solids Struct, 46 (2009) 1413-1422.
[37] Q.H. Fang, H. Feng, Y.W. Liu, S. Lin, N. Zhang, Special rotational deformation effect on the emission of the dislocations from a crack tip in deformed nanocrystalline solids. Int J Solids Struct, 49 (2012) 1406-1412.
[38] T.Y. Zhang, J.C.M. Li, Image forces and shielding effects of an edge dislocation near a finite length crack. Acta Metall Mater, 39 (1991) 2739-2744.
[39] J.P. Hirth, J. Lothe, Theory of dislocations, second ed, John-wiley, New York, 1964.
[40] J.R. Rice, R. Thomson, Ductile versus brittle behaviour of crystals. Philos Mag, 29 (1974) 73.
[41] J.P. Hirth, J. Lothe, Tgeiry of dislocations, Wiley, New York, 1982.
[42] M.X. Huang, Z.H. Li, Dislocation emission criterion from a blunt crack tip. J Mech Phys Solids, 52 (2004) 1991-2003.